

## AN EXPERIMENTAL AND NUMERICAL CFD STUDY OF TURBULENCE IN A TUNDISH CONTAINER

P. GARDIN<sup>1</sup>, M. BRUNET<sup>1</sup>, J.F. DOMGIN<sup>1</sup> and K. PERICLEOUS<sup>2</sup>

<sup>1</sup> IRSID Groupe Usinor, Maizières-lès-Metz, FRANCE

<sup>2</sup> University of Greenwich, London SE18 6PF, ENGLAND

### ABSTRACT

This paper describes work performed at IRSID/USINOR in France and the University of Greenwich UK, to investigate flow structures and turbulence in a water-model container, simulating aspects typical of metal tundish operation. Extensive mean and fluctuating velocity measurements were performed at IRSID using LDA to determine the flowfield and form the basis for a numerical model validation.

This apparently simple problem poses several difficulties for the CFD modeling. The flow is driven by the strong impinging jet at the inlet. Accurate description of the jet is the most important and requires a localized fine grid, but also a turbulence model that predicts the correct spreading rates of jet and impinging wall boundary layers. The velocities in the bulk of the tundish tend to be (indeed need to be) much smaller than those of the jet, leading to damping of turbulence, or even laminar flow. The authors have developed several low-Re  $k$ - $\epsilon$  model variants to compute this flow and compare against measurements. Best agreement is obtained when turbulence damping is introduced to account not only for walls, but also for low Re regions in the bulk - the  $k$ - $\epsilon$  model otherwise allows turbulence to accumulate in the container due to the restricted outlet. Several damping functions are tested and the results reported here. The  $k$ - $\omega$  model, which is more suited to transitional flow, also seems to perform well in this problem.

### NOMENCLATURE

$a$	characteristic length
$p$	pressure
$\mathbf{u}$	velocity
$\rho$	density
$k$	turbulent kinetic energy
$\epsilon$	dissipation rate of $k$
$\omega$	frequency of the vorticity fluctuations
$\mu$	dynamic viscosity

### INTRODUCTION

In steel-making processes, most flows are confined. Movement of liquid steel is created by gas plumes (ladles or RH vacuum degasser), or by jets entering the reactor (tundish and continuous casting mold). The flow regime is mostly turbulent, but some turbulence attenuation can occur far from the inlet(s). Characteristic hydrodynamic situations include: jet spreading, jet impingement on the wall, wall jets and important decrease of turbulence intensity in the core region of the reactor far from the jet. In the case of the tundish, the inlet velocity is about 1 m/s, whilst

typical bulk velocity may be less than 1 cm/s, to promote flotation of inclusions.

For a CFD code, it is a challenge to correctly mimic the flow behavior for such systems (Gardin et al., 1997, Mysco et al., 1996). Although most of the research teams acting for flow prediction in a tundish use CFD codes, validation of numerical results is scarce and there is a lack of guidelines for proper predictions. Exception is Chakraborty et al. (1987, 1991), who clearly established that care has to be taken in order to get reliable numerical results, especially for Residence Time Distribution.

This paper is devoted to the test of different 2-equation turbulence models, making the comparison with measurements performed in a water model.

### Description of the Water Model

The water model represents the main aspects of flow in a tundish (Figure 1): jet spreading, impingement on wall and progressive decrease of turbulence when flow comes near the outlet. To simplify the measurements, there is no wall inclination and the free surface present in real systems is replaced with a wall. Reynolds similarity is used. Because the incoming turbulence and velocity profile have major influence on jet spreading, a long entrance pipe was built: there is a progressive forgetting of the inlet boundary conditions along this pipe, avoiding having precise inlet boundary conditions for turbulent quantities (inlet velocity is 1.38 m/s). Velocity measurements were performed by 1-component Laser Doppler Anemometer.

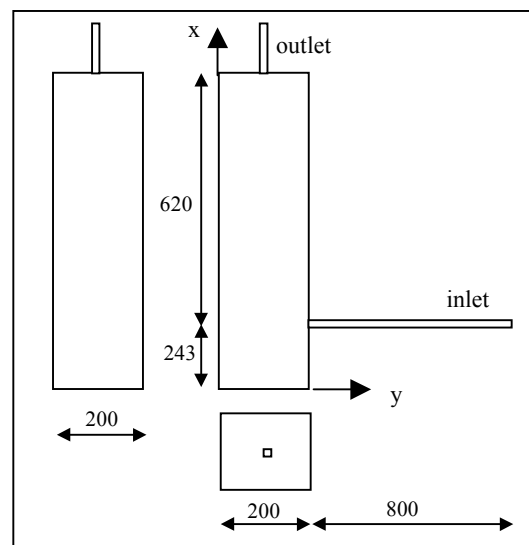


Figure 1: The IRSID water model

## MATHEMATICAL MODEL

The flow in the tundish was computed numerically using the finite-volume CFD code PHOENICS. This section will highlight the equations used, relevant to the modeling of turbulence and their modification for tundish simulation. It is useful for reference to introduce the transport equation (1), for a generic variable  $\phi$ , which is used for all conserved variables in a fluid flow problem, including mass, momentum and the turbulence variables  $k$ ,  $\epsilon$  and  $\omega$ :

$$\frac{\partial(\rho\phi)}{\partial t} + \text{div}(\rho \mathbf{u} \phi - \Gamma_\phi \text{grad} \phi) = S_\phi \quad (1)$$

The LHS terms in the equation represent time accumulation, transport by convection and diffusion. The RHS represents source or sink terms,  $S_\phi$  appropriate to each  $\phi$  equation. The diffusion coefficient  $\Gamma_\phi$  is specified to be the sum of viscous and turbulent contributions and requires a turbulence model for its determination.

The water flow in the model tundish is incompressible and isothermal; this latter point is questionable: buoyancy effect may occur in low velocity parts of a tundish due to heat flux extraction from the walls, but there is no special difficulty taking this effect into account in CFD code. It is assumed that the flow is also time-independent; hence the transient term in equation (1) is neglected in these computations (note that the last assumption is not necessary, but adopted to reduce computational cost).

Two classes of turbulent models have been applied and evaluated in this study. The first based on the  $k$ - $\epsilon$  model of Launder and Spalding (1974), the second based on the  $k$ - $\omega$  model of Wilcox (1994). Modifications have been introduced to address the specific flow regime encountered in the experiment.

### (1) The $k$ - $\omega$ model of Wilcox

This model solves for the kinetic energy of turbulent fluctuations (per unit fluid mass),  $k$  and  $\omega$ , the frequency of the vorticity fluctuations. The basic equations are (Wilcox, 1998):

$$\frac{\partial(\rho u_i k)}{\partial x_i} - \frac{\partial}{\partial x_i} \left[ (\mu + \sigma_k^* \mu_t) \frac{\partial k}{\partial x_i} \right] = \rho G - \beta^* \rho \omega k \quad (2)$$

$$\frac{\partial(\rho u_i \omega)}{\partial x_i} - \frac{\partial}{\partial x_i} \left[ (\mu + \sigma_\omega \mu_t) \frac{\partial \omega}{\partial x_i} \right] = \rho \alpha \frac{\omega}{k} G - \beta \rho \omega^2 \quad (3)$$

The RHS of equations (2) and (3), contains a source term matched by a sink term. The balance of these terms determines whether turbulence will be generated or destroyed at any point in the flow. The quantity  $G$ , responsible for the production of turbulent energy is modeled by the following expression:

$$G = -\overline{u_i' u_j'} \frac{\partial u_i}{\partial x_j} \approx v_t \left( \frac{\partial u_i}{\partial x_j} + \frac{\partial u_j}{\partial x_i} \right) \frac{\partial u_i}{\partial x_j} \quad (4)$$

The Reynolds stresses have been represented by the isotropic scalar turbulent viscosity  $\nu_t$ , which is then added to the laminar viscosity to form an effective diffusion coefficient in equations (1)-(3). The turbulent viscosity is then given by,

$$\mu_t = \alpha^* \rho k / \omega \quad (5)$$

The model has various constants and other quantities that are a function of the local turbulent Reynolds number. These were introduced to enable satisfactory performance close to walls and elsewhere, where viscous dissipation becomes important. Table 1, gives the values of these constants taken from Wilcox (1998) and used in this implementation. This model was shown to be able to predict transition from laminar to turbulent flow, in boundary layers and ducts. The high Re version can be recovered by setting the turbulent Reynolds number,  $R_t$  to  $\infty$ . In contrast to other 'low-Re' models, the wall distance is not required by this model, except in the wall boundary conditions. Nevertheless, the values of the closure constants have been determined by reference to the growth of instabilities in the boundary layer. It is not certain therefore, how accurate this model is, away from the wall regions.

Wall boundary conditions are required for equations (2) and (3). These are,

$$k = 0 \text{ and } \omega \rightarrow \frac{6\nu}{\beta y^2} \text{ as } y \rightarrow 0 \quad (6)$$

There is some controversy regarding the asymptotic behaviour of  $\omega$  as the wall is approached, in that equation (6) implies,  $\tau_{xy} \sim y^4$ , whilst theory shows that  $\tau_{xy} \sim y^3$ . Finite volume implementation in the PHOENICS code requires fixing the boundary values at the node nearest to the wall to those of equation (6). This approach gave good results in two classical 2D benchmark problems, (i) the backward-facing step, (ii) the impinging slot-jet with heat transfer (Gardin (1997), Tilford (1999)).

Variable	Expression/Value
$\sigma_k^*, \sigma_\omega$	1/2
$\beta$	3/40
$\alpha$	$\frac{5}{9} \frac{\alpha_0 + R_t^* / R_\omega}{1 + R_t^* / R_\omega} (\alpha^*)^{-1}$
$R_t^*$	$\rho k / (\omega \mu)$
$\beta^*$	$\frac{9}{100} \frac{5/18 + (R_t^* / R_\beta)^4}{1 + (R_t^* / R_\beta)^4}$
$\alpha_0$	1/10
$\alpha^*$	$\frac{\alpha_0^* + R_t^* / R_k}{1 + R_t^* / R_k}$
$\alpha_0^*$	$\beta/3$
$R_\beta$	8
$R_k$	6
$R_\omega$	2.7

**Table 1:** Expressions used in the  $k$ - $\omega$  model

Other implementations (e.g. the code CFL3D) suggest that a multiple of expression (6) may be preferable :

$$\omega_w = \frac{60\nu}{\beta y_w^2} \quad (7)$$

This formulation was found to give improved results in the 3-D tundish problem, but generality of this expression is questionable.

## (2) The k-ε model

The high Reynolds number version of this model (Launder & Spalding (1974)) is by far the most widely used turbulence model for industrial applications and it remains the standard model in all CFD codes. The model is known to have many drawbacks and for this reason there are many variants of it, which have proved successful in producing case-specific improvements. Many of these 'improvements' often are no more than attempts to counter the drawbacks of the fundamental assumption of isotropy. For example, correction coefficients have been introduced to account for vortex stretching due to a body force or due to streamline curvature. More generic improvements though have been introduced to enable the model to work in low-Re, or transitional flow regimes. These will be discussed further here, since they affect tundish-type flows.

In the k-ε model, ω is replaced by the rate of turbulent eddy dissipation, ε. The two quantities are related by the expression,

$$\varepsilon = \beta^* k \omega \quad (8)$$

The k-ε transport equations are then simply a transformation of (2) and (3) above:

$$\frac{\partial(\rho u_i k)}{\partial x_i} - \frac{\partial}{\partial x_i} \left[ \left( \mu + \frac{\mu_t}{\sigma_k} \right) \frac{\partial k}{\partial x_i} \right] = \rho G - \rho \varepsilon \quad (9)$$

$$\frac{\partial(\rho u_i \varepsilon)}{\partial x_i} - \frac{\partial}{\partial x_i} \left[ \left( \mu + \frac{\mu_t}{\sigma_\varepsilon} \right) \frac{\partial \varepsilon}{\partial x_i} \right] = f_1 \rho C_1 \frac{\varepsilon}{k} G - f_2 C_2 \rho \frac{\varepsilon^2}{k} \quad (10)$$

The eddy viscosity is given as,

$$\mu_t = f_\mu C_\mu k^2 / \varepsilon \quad (11)$$

The standard model constants are,

$$C_\mu = 0.09, C_1 = 1.44, C_2 = 1.92. \quad (12)$$

This model is presented in the low Reynolds number form, containing the viscous damping function multipliers,  $f_1$ ,  $f_2$  and  $f_\mu$ . These functions become equal to 1.0 when the Reynolds number is large. They are mostly the result of asymptotic solutions in the boundary layer regions of the flow and as such they are by no means universal. In fact, there are probably as many variants as there are turbulence researchers.

## Turbulence Model Modifications

Initial tundish computations performed in IRSID (1998), using the standard high-Re k-ε model in PHOENICS highlighted several problems:

- The jet appeared to spread much faster than the experimental one, leading to accelerated decay of the maximum velocity.
- The jet appeared to deviate slightly towards the outlet, whilst the experimental jet did not.
- There was a worrying discrepancy in the axial velocity profiles, when axial traverses of this component were plotted at a small distance from the impingement wall.

These differences between experiment and computation, plus the fact that the prevailing Reynolds number away from the jet was close to the critical value of 2000 (critical value for a pipe flow, which is not, however, exactly the situation here), led us to believe that the turbulence predicted by the k-ε model was far too high. The over-spreading of the jet of course could be due to other factors, i.e. the coarseness of the mesh, or the well-known deficiency of all 2-equation models in this respect (see Myzsko et al., 1996). Later computations by IRSID, using a range of meshes, showed indeed that mesh refinement can improve the jet behaviour considerably, although even the finest mesh still gave too rapid a decay of jet centre-line velocity. The finest mesh also allowed the use of a low-Re version of the k-ε model, specifically the Chen-Kim (1987) variant. The best results were obtained with this model, although significant discrepancies remained.

Two-dimensional parametric studies indicated that part of the problem is the "swamping" of the jet shear generated turbulence by entrained bulk turbulence accumulated in the enclosed regions either side of the jet - a viscous damping problem.

Viscous damping is taken care of by the damping functions mentioned earlier, which feature in both the k-ε and k-ω type models. These functions have been "tuned" so that they satisfy universal boundary layer profiles (see Wilcox (1994)) and also to work asymptotically in long ducts for turbulent decay behind a grid. Therefore the situation presented here, which features elliptic conditions for turbulence is a severe test for these models. Bearing this in mind, the following alternative modifications were introduced to the standard k-ε model to account for viscous damping away from walls:

### Option D1,

$$f_\mu = \min [1, a R_t^b] \\ a = 1/45, b = 1/3, R_t = \frac{\rho k^2}{\mu \varepsilon} \quad (13)$$

### Option D2,

$$f_\mu = 1 - \exp \left\{ - \frac{R_t}{25 \sqrt{3/2}} \right\} \quad (14)$$

### Option D3

$$f_\mu = \exp \left\{ \frac{-3.4}{(1 + R_t / 50)^2} \right\} \quad (15)$$

Option D2 is inspired from the Launder-Sharma (1974) formula and option D3 is a generalization of the Van Driest exponential decay formula for viscous dissipation away from walls, with the turbulent Reynolds number replacing the wall distance Reynolds number  $Y^+$ . Option D1 attempts to capture features of both models. The three expressions are compared in Figure 2. The identifiers D1, D2 and D3 will be used in the plots of results to signify the use of each model.

To also account for wall proximity, option D1 was modified, so that the eddy viscosity becomes :

$$\mu_t = \min [1, a R_t^b] \left( 1 - \exp(-Y^+ / 25) \right)^2 \frac{\rho k^2}{\epsilon} \quad (16)$$

These modifications were found to have a significant effect in the distribution and magnitude of turbulence in the container.

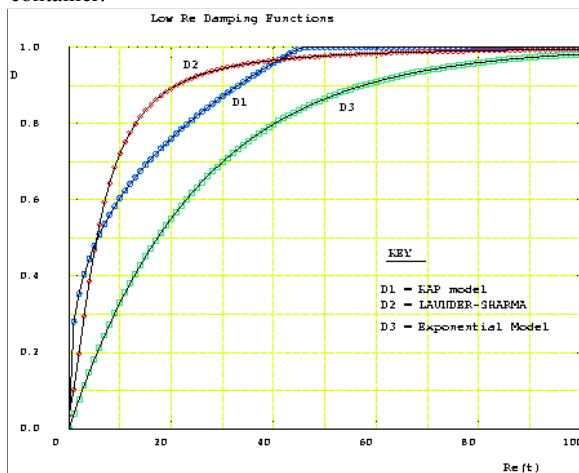


Figure 2: Damping functions

### Problem Setup and Computer Requirements

The container shown in Figure 1, was modeled using the PHOENICS code. The inlet and outlet tubes were not included in the computation with the calculation domain only covering the main container. To account for velocity and turbulence variation at the inlet, a separate computation of the square inlet duct velocity field was conducted using a fine (50x50) mesh over a quarter of the duct section. The resulting turbulent profiles of velocity,  $k$  and  $\epsilon$  were used as boundary conditions at the inlet. By symmetry, only half the container was modeled. A non-uniform Cartesian mesh was used, with a power-law expansion of cells from the walls outwards. The finest cells were placed next to the jet-impact wall, since that is where maximum resolution was needed for the fast moving boundary layers. A fine mesh was also used to cover the jet region. Three different mesh densities were used which will be referred to as, the Coarse (48x30x16), Medium (52x34x20) and Fine (104x68x40) meshes. So, a total of about 283 000 cells were used in the finest calculation.

A steady-state incompressible solution procedure was adopted, with the main dependent variables being the pressure (mass), three velocity components and the two turbulent quantities. The pressure was solved using a whole-field 3D solver, whilst all other quantities used a slab-wise solver. Hybrid differencing was used to convert the partial differential equations (1)-(3) into finite-volume equivalents.

Inertial false-time-step relaxation was used for the momentum equations, based on average cell residence time ( $\delta t_i=0.1s$ ). Slightly heavier relaxation was used for the turbulence quantities. Convergence was generally monotonic or all turbulence models, requiring between 1000 and 3000 sweeps. Of the  $k-\epsilon$  models tried, D1 appeared to converge fastest based on the residual printout, whilst D3 was the slowest. Parametric solutions were usually obtained by ‘restarting’ the calculation from a previous model, to speed up convergence. For the Medium grid, 3.3 CPU-hours were needed, to compute 1000 sweeps of the problem on a 166Mhz Pentium PC. Fine grid runs were performed on a SUN Ultra workstation.

Table 2 displays the matrix of 3D runs performed, to compare the various models. It should be noted that the ‘Coarse’ mesh was only used in preliminary computations and then abandoned.

Run #	Model	Grids
1	$k-\omega$	C/M/F
2	$k-\epsilon$ -HRN	C/M/F
3	$k-\epsilon$ -D1	M/F
4	$k-\epsilon$ -D2	M/F
5	$k-\epsilon$ -D3	M/F
6	$k-\omega$ -60	M/F

Table 2: Matrix of runs

## RESULTS

Typical results are given graphically in the attached figures (3-7). These compare the mean velocities and some RMS turbulence values against the experimental data provided by IRSID .

### (a) Mean velocities

Due to lack of space only a small sample of the results is given here. Of all the  $k-\epsilon$  variants, the D1 version gave the best agreement with experiments. This is compared with the  $k-\omega$  model in the plots, for the fine mesh runs only. Figure 3 first, shows the jet velocity profile close to the inlet. Both the  $k-\epsilon$ -D1 and  $k-\omega$  model show good agreement with measurements. Figure 4 shows that even much further downstream, close to the impact wall, the velocity profile is represented reasonably well, with the  $k-\omega$  model being marginally better. The rate of jet centerline velocity decay can be seen in Figure 5. Again here agreement is good, with discrepancies being greater close to the impact wall.

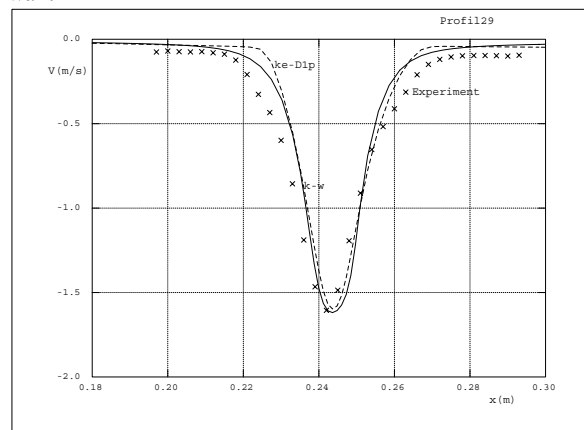


Figure 3: Jet velocity profile close to inlet

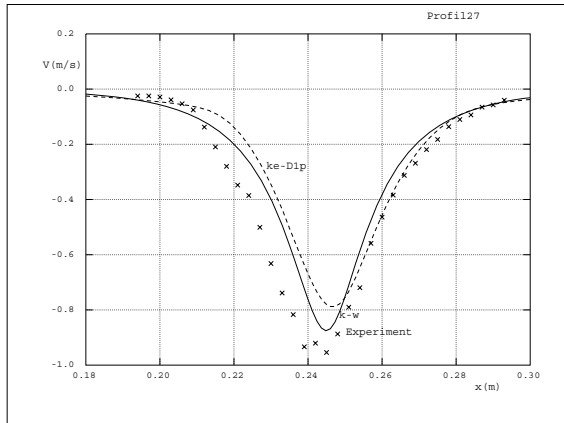


Figure 4: Jet velocity profile close to wall

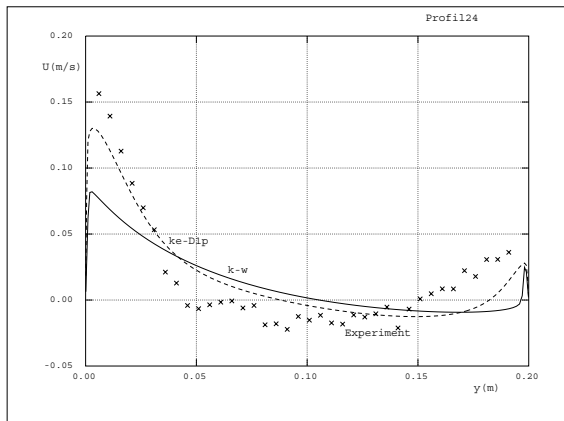


Figure 5: Jet centerline decay

**(b) Turbulent quantities**

The object of this study is to investigate the influence of turbulence models in tundish flows. The measured RMS values of turbulent velocity were compared against the computed values of  $k$ . Unfortunately only two velocity components ( $U_{rms}$  and  $V_{rms}$ ) were measured, which made direct comparisons impossible (since  $k = 0.5 \cdot (u^2 + v^2 + w^2)$ ,  $u$ ,  $v$  and  $w$  being the unknown velocity fluctuations). It can be taken that  $U_{rms} = \sqrt{u^2}$  and  $V_{rms} = \sqrt{v^2}$ . Then, the mean (or isotropic) fluctuation  $U_{mean} = \sqrt{2k/3}$ . Also, all two-equation models assume isotropy of turbulence, i.e. the velocity fluctuations are supposed to be equal in magnitude. A quick inspection of the measurements reveals that in the jet region,  $V_{rms} \sim 2-3 \cdot U_{rms}$ . Despite these uncertainties certain useful deductions can be drawn from the results, a sample of which is included here.

Figure 6 shows measured  $U_{rms}$  across the duct ( $y$ -direction) against the equivalent fluctuations ( $U_{mean}$ ) obtained from the  $k$  field. Experiments M21 – M24 are depicted on the graph, representing various positions inside and down-stream of the jet. A high turbulence regime (M22, M23) exists near the jet, a low turbulence regime (M24) well downstream of the jet, and experiment M21 through the jet axis, where turbulence varies from low values at the inlet to high values towards the wall. These transitions are fairly well represented by the turbulent models used. The main difference between the standard  $k-\epsilon$  and the modified one being in this case the variable M21 regime. The D1-variant gives the jet a longer potential

core, in contrast to the standard  $k-\epsilon$  which suppresses this core, then increasing radial diffusion of momentum and decreasing axial velocity. The truth lies between these two extremes.

Figure 7 compares the  $V_{rms}$  values close to the jet inlet with the ones predicted by the two models. The profiles indicate a low turbulence region in the jet core and high turbulence generated by the shear layers (where the mean velocity gradient is a maximum). The  $k-\epsilon$  D1 model seems to underpredict turbulence levels outside the jet whilst the  $k-\omega$  model slightly overpredicts the fluctuations.

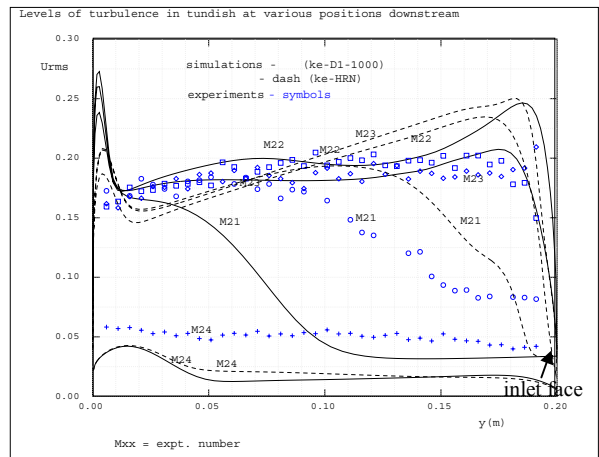


Figure 6: Turbulence levels at various positions in the tundish

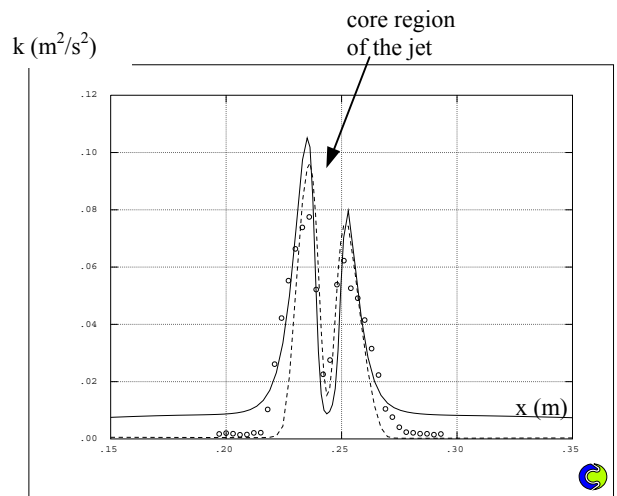


Figure 7: Turbulence close to the inlet

**CONCLUDING REMARKS**

This work started with the objective of applying and validating the  $k-\omega$  model of Wilcox to a tundish flow problem. This model was thought to have advantages over the industrial standard  $k-\epsilon$  model, which IRSID had already used for this problem with mixed success.

After initial 2D studies, it was found that the  $k-\omega$  model was diffusing the jet too quickly. Medium grid density 3D computations (run to the limit of the PC computer used), confirmed this finding. Study of the numerical results

suggested that turbulence was accumulating in the mostly enclosed tundish and then entrained into the jet dissipating its momentum. Ways were sought to damp turbulence in the low Reynolds number regions of the flow away from the walls. Modifications were introduced to both k- $\epsilon$  and k- $\omega$  models to this effect. These appeared to be successful and the grid was refined by a factor of 8, to a maximum of 280 000 cells, to perform parametric studies.

The k- $\epsilon$  modifications proved very successful, with the newly developed k- $\epsilon$ -D1 model being the best. The grid refinement also showed that certain turbulence models were more grid-sensitive than others. Accurate representation of the inlet velocity and turbulence profiles had an influence on the solutions close to the jet, but a less marked effect elsewhere.

## REFERENCES

- M. BRUNET, (1998), IRSID private communication.  
CFL3D code manual, NASA Langley CFD section <http://fmad-www.larc.nasa.gov/~rumsey/CFL3D/>
- S. CHAKRABORTY, Y. SAHAI, (1987), "The effect of tundish wall inclination on the fluid flow and mixing : a modeling study", *Metallurgical Transactions B*, **18B**, 81-92
- S. CHAKRABORTY, Y. SAHAI, (1991), "Role of near-wall location on the prediction of melt flow and residence time distribution in tundishes by mathematical modelling", *Metallurgical Transactions B*, **22B**, 429-436.
- C.J. CHEN, S.Y. JAW, (1998), "Fundamentals of Turbulence Modelling", *Taylor-Francis*.
- Y.S. CHEN & S.W. KIM, (1987), "Computation of turbulent flows using an extended k- $\epsilon$  model", *NASA rep. CR-179204*.
- P. DURBIN, (1995), "Separated flow computations with the k- $\epsilon$ - $u^2$  model", *AIAA Journal*, **33**(4).
- P. GARDIN, K. PERICLEOUS, (1997), "Heat transfer by impinging jets on a moving strip", Proc. CSIRO CFD conf., Melbourne.
- B. LAUNDER & B. SHARMA, (1974), "Application of an energy dissipation models of turbulence near a spinning disk", *Letters in Heat and Mass Transfer*, **1**, pp 131-138.
- B. LAUNDER & D.B. SPALDING , "The numerical modelling of turbulent flows", *Comp. Methods in appl. Mech. and engng.* **3**, pp 269-289, 1974.
- M. MYZSCO & K. KNOWLES, "Numerical modelling of a single impinging jet and experimental validation" *PHOENICS Journal*, vol 9,1, pp 51-60, 1996.
- POLIS "The PHOENICS on line help facility", CHAM ltd, Wimbledon
- W. RODI , (1980), "Turbulence models and their application in hydraulics", *IAHR*, Delft.
- T. TILFORD, "Advanced turbulence models" MSc Thesis, University of Greenwich, 1999.
- A.R.P. VAN HEININGEN "Heat transfer under an impinging jet", *PhD Thesis, McGill Univ.*, 1982
- J.C. VOGEL & EATON, (1984), "Heat transfer and fluids mechanics measurements in the turbulent reattaching flow behind a backward-facing step", *Rep. MD-44, Mech. Eng., Stanford Univ., CA*.
- D.C. WILCOX, (1994), "Simulation of transition with a two-equation turbulence model", *AIAA Journal*, **32**(2).
- D.C. WILCOX, (1998), "Turbulence modelling for CFD" , DCW Industries, La Canada CA.